

### **JGR** Atmospheres

#### **RESEARCH ARTICLE**

10.1029/2018JD029920

#### **Special Section:**

A New Era of Lightning Observations From Space

#### **Key Points:**

- Global and regional long-term trends in thunder days are determined at ground stations
- Largely positive correlations are observed between the simultaneous thunder-day and TRMM-LIS lightning flash density trends throughout the tropics and subtropics
- Regions of disagreement in the relationship between trends in thunder days and flash density, all have negative or no correlation between the number of thunderstorms and the number of flashes/LPF

#### Correspondence to:

T. Lavigne, tlavigne@islander.tamucc.edu

#### Citation

Lavigne, T., Liu, C., & Liu, N. (2019). How does the trend in thunder days relate to the variation of lightning flash density? *Journal of Geophysical Research: Atmospheres*, *124*, 4955–4974. https://doi.org/10.1029/2018JD029920

Received 30 OCT 2018 Accepted 26 MAR 2019 Accepted article online 2 APR 2019 Published online 6 MAY 2019

#### **Author Contributions:**

Conceptualization: Thomas Lavigne, Chuntao Liu, Nana Liu Data curation: Chuntao Liu Formal analysis: Thomas Lavigne, Nana Liu Funding acquisition: Chuntao Liu

Methodology: Thomas Lavigne, Chuntao Liu, Nana Liu Resources: Chuntao Liu Supervision: Chuntao Liu

Writing - original draft: Thomas Lavigne

Writing – review & editing: Chuntao Liu, Nana Liu

©2019. American Geophysical Union. All Rights Reserved.

## How Does the Trend in Thunder Days Relate to the Variation of Lightning Flash Density?

Thomas Lavigne<sup>1</sup>, Chuntao Liu<sup>1</sup>, and Nana Liu<sup>1</sup>

<sup>1</sup>Department of Physical and Environmental Sciences, Texas A&M University-Corpus Christi, Corpus Christi, TX, USA

**Abstract** A longstanding question for scientists has been whether or not any observable trends or shifts in global lightning activity have occurred since the Industrial Revolution. This study utilized over 8,000 certified ground-based stations over a 43-year period, as well as 16 years of Tropical Rainfall Measuring Mission (TRMM) Lightning Imaging Sensor (LIS) data, to provide a better understanding of the processes behind these trends. Ground station results show that many global regions have observed significant increases or decreases in thunder day occurrence. The Amazon, Maritime Continent, India, Congo, Central America, and Argentina display increases in annual thunder days since the 1970s, whereas China, Australia, and the Sahel among others observe decreases in the number of thunder days. The corresponding change in lightning flash density from the TRMM-LIS, as well as the number of thunderstorm features and lightning flashes per thunderstorm feature, is compared to the thunder day trends during the TRMM lifespan. Results show a positive correlation between the changes of thunder day occurrence and flash density over most regions of the TRMM domain, including the Maritime Continent, China, South Africa, and Argentina. However, there are several regions with disagreements between the flash density and thunder day trends, such as India and Western Africa. The disagreements are related to the changes in the number of flashes per thunderstorm, which suggest other reasons to interpret the long term trends in thunder day occurrence over various regions. Understanding these regional trends in lightning activity is important in understanding the changes of precipitation systems under a varying climate.

#### 1. Introduction

For decades, a longstanding question for scientists has been if any observable trends or shifts in global lightning activity have occurred since the Industrial Revolution and beyond (Changnon, 1985). It has been hypothesized that for every increase in air temperature of 1 °C, global lightning activity would increase by approximately 5–%6% (Price & Rind, 1994) or 11% (Williams, 2012), which indicates that the warming of the planet should lead to an increase in global lightning.

A team of scientists has recently been established to make lightning data available for use in understanding the changing climate (Aich et al., 2018). The lightning variable has been shown to have a close relationship with thunderstorm activity, as well as precipitation patterns (Price, 2013; Williams, 2005). Recently, the electrical properties of clouds and precipitation systems have become increasingly useful for understanding the changes and shifts in global climate and have been added to the Global Climate Observing System's list of essential climate variables. The major shortcoming of the use of past lightning activity to monitor climate is the relatively short time span of measurement, as well as limited global observations. For these reasons, lightning proxy data sources, such as the thunder day variable, have been identified as an important data set for examining the changing climate, due to its relative long-term record, as well as near-global land coverage (Aich et al., 2018). One goal of this study is to better understand what the thunder day variable represents in the context of number of thunderstorms and flash density and to possibly use this information to quantify the trends in lightning around the globe.

According to the historical works by Brooks (1925), as well as the World Meteorological Organization, a thunder day is defined as a local calendar day on which thunder is heard (World Meteorological Organization, 1953). A thunder day is recorded as such regardless of the actual number of thunderstorms occurring on that day. When a storm begins before midnight and ends after midnight, two thunderstorm days are recorded (World Meteorological Organization, 1953). This is possible during long-lived nocturnal mesoscale convective systems (MCS), which can span across midnight, into a second day. Various localized studies have been conducted on the frequency of thunder days, and other severe weather phenomena, using



ground station data on the annual and seasonal time scales. These regional studies have revealed that the tendency of thunder days in the past century has been highly variable and regionally specific. In Asia, Lin-Lin et al. (2010) and Zhang et al. (2017) presented that the occurrence of weather events such as thunderstorms and hail have been decreasing in China in the past 50 years. Zhang et al. (2017) showed that based on over 500 ground stations covering China, there has been a decrease in thunder and hail days by approximately 50% since 1960. This decrease in thunder day incidence was linked to the simultaneous downturn in intensity of the Asian Summer Monsoon and has been accompanied by the presence of smaller hail size, which also indicates weakening convection in the region (Ni et al., 2017). Kitagawa (1989) exhibited that over the past 100 years, the frequency of winter thunder days has increased along the coastal ground stations of Japan. During the same period of time, the inland plains ground stations showed a decrease in thunder day frequency during the summer. In Southern Asia, the Island of Sri Lanka has shown a predominantly increasing long-term trend in thunder days annually (Sonnadara, 2016). This study, which made use of nine ground-based stations across the country during the years of 1961-2010, showed that five stations had a significant increase in annual thunder days, while four showed no significant trends. This rules out the presence of a large-scale thunder day trend across Sri Lanka but could emphasize the importance of smaller-scale topography and monsoonal direction.

In Europe, Enno et al. (2014) showed a significant decrease in thunder day occurrence of approximately 24% in the Baltic Region, including the countries of Estonia, Latvia, and Lithuania, at 40 stations between the years of 1950 and 2004. The study linked the decrease in annual thunder days to an increasing number of northerly circulation type weather events, which are thought to have decreased the likelihood of severe weather in the region. Another study conducted in Northern Eurasia concluded that days observing convective precipitation have increased in all seasons during the time period of 1966–2000 (Ye et al., 2017). The study showed that the increasing trends were highly correlated with surface warming and moistening that might have contributed to an increase in Convective Available Potential Energy and a subsequent decrease in stability in the region. Another study in Finland exhibits the ability to compare the annual number of thunder days, to the cloud-to-ground lightning flash density (Tuomi & Mäkelä, 2008). The estimated flash density using lightning flash counters exhibits a very similar interannual variability to that of annual thunder days, indicating the possibility of using the number of thunder days as a proxy for flash density in some regions.

In the Americas, Pinto et al. (2013) revealed an increasing trend in annual thunder days in Southeast Brazil. Since the nineteenth century, the cities of Compinas and Sao Paulo have demonstrated significant increases in number of annual thunder days (68% and 40% increases, respectively). This increase was linked to the industrialization and growing urbanization in these cities in the twentiethh century (Pinto et al., 2013). Changnon and Changnon (2001) reported on the 100-year trends in lightning activity in the United States. Their results showed that the region is highly variable in annual thunder day occurrence from 86 stations, with 31 stations showing no trend, 26 showing decreasing trends, and 31 stations observing increasing trends. However, it is still not clear how to interpret these thunder day changes in the perspective of the variation of thunderstorm and lightning activity. This study did not emphasize the occurrence of the "Big Hiatus" during 1940–1975, in which the trend in global temperatures flattened out substantially, with the associated thunder day trends decreasing in occurrence. This time period could influence the trend analysis and partially explain the lack of substantial trends in the United States during this study.

Results from these regional ground station studies of long-term thunder day trends show that unique regional mechanisms can influence the trends in localized thunder day frequency. Each individual region has its specific convectively active time period, which contributes to the global summation of lightning activity. Understanding how these time periods are changing globally can allow us to study the changes in global lightning at different time scales. Long-term global shifts in thunderstorm activity could subsequently shift the diurnal and seasonal distribution of global lightning. It is important to monitor these shifts in thunder days and flash density at the global scale, in order to observe the impacts on Earth's electrical processes (Williams, 2009). These processes such as the global electric circuit of the atmosphere are driven by electrified cloud parameters at the diurnal and seasonal timescales (Adlerman & Williams, 1996; Blakeslee et al., 2014; Lavigne et al., 2017; Liu et al., 2010; Williams, 1994; Williams & Heckman, 1993). Changnon (1985) attempted to observe global shifts in thunder day frequencies using 227 ground-based stations. This study builds upon the regional and global works that have been conducted in the past and gives a more



comprehensive look at the changes observed in global lightning, which could possibly help to understand the global variability of the Earth's electrical systems in the past and into the future. One important global study was conducted utilizing lightning flash counters to approximate the lightning flash rate across a significant portion of the globe (Mackerras et al., 1998). The study shows how total lightning flash density varies across different latitudes, seasonally and diurnally, and serves as an important baseline for the global lightning flash density climatology prior to satellite technology.

The Tropical Rainfall Measuring Mission-Lightning Imaging Sensor (TRMM-LIS) has been used in the past in numerous studies to help understand the spatial and temporal distribution of lightning and thunderstorms (Albrecht et al., 2016; Cecil et al., 2005; Christian et al., 1999; Liu et al., 2012; Toracinta et al., 2002; Zipser et al., 2006). Studies such as these have been very successful at determining the most convectively active regions of the world and with the most lightning activity. The TRMM-LIS has also been used to show the diurnal variability of lightning (Cecil et al., 2005). This study showed that over most land regions, the peak in diurnal activity occurred in the late afternoon (approximately 1600 local time), whereas over the ocean, a much smaller diurnal amplitude was observed, with the peak in the early morning (approximately 0300 local time; Williams et al., 2000). The TRMM-LIS has also been used to monitor the regional effects of El Niño–Southern Oscillation (ENSO) on lightning activity (Chronis et al., 2008; Hamid et al., 2001; Sátori et al., 2009; Williams, 2012; Yoshida et al., 2007). These findings show that natural climate variability can be observed by the TRMM satellite.

This study compares ground-based station thunder day data, to the flash density and population of thunder-storm records from the TRMM satellite. The comparison of the global trends observed in the thunder day occurrence, to the trends observed in lightning flash density (flashes/km $^2$  × year), and population of thunderstorms gives us a more complete understanding of the trends and tendencies in global lightning activity. It also provides an opportunity to observe the capabilities of the TRMM-LIS in observing regional trends in lightning activity compared to ground-based station observations.

Although the 16-year time series (1998–2013) is not long enough to establish robust climatological trends, it is still worthwhile to investigate whether the trends in thunder day occurrence and trends in TRMM-LIS flash density are consistent during the 16-year period. The motivation of this study is to answer the following questions:

- 1. Are any regional trends observed in the long-term thunder day occurrence from the ground stations?
- 2. What are the long-term annual and seasonal trends in thunder day occurrence in some of the most convectively active regions of the globe?
- 3. Is there any agreement in the ground station thunder day occurrence trends and the lightning flash density observed by the TRMM satellite during the TRMM timespan of 1998–2013?
- 4. Is there any way that we can explain the similarities and differences in these trend values over different regions by examining the properties of thunderstorms?

To answer these questions, this study builds upon past regional thunder day studies, with a more robust quantity of global stations, as well as the use of the 16-year TRMM-LIS observations. Section 2 introduces the data sets and methodology that were used. Section 3.1 looks into the long-term annual trends in thunder days observed by the ground stations, followed by section 3.2, which looks at the thunder day trends seasonally. Section 3.3 examines the spatial correlation of the ground station thunder days and the satellite flash density as well as population of thunderstorms, while section 3.4 compares and contrasts the trends observed by the three variables. Section 4 discusses the results, and section 5 summarizes the important findings.

#### 2. Data and Methodology

#### 2.1. Global Surface Summary of the Day

The Global Surface Summary of the Day (GSOD) is a data set of over 9,000 ground-based meteorological stations located worldwide (https://data.nodc.noaa.gov/). This data set is organized and quality controlled by the National Oceanic and Atmospheric Administration (NOAA). The daily ground station data includes meteorological measures such as mean temperature, minimum temperature, maximum temperature, dew point, station pressure, wind speed, visibility, and precipitation amount. The data set also has occurrence

flags for each day indicating the binary occurrence of fog, rain, snow/sleet, hail, thunder, and tornadoes. For the purpose of this study, only the binary occurrence of thunder days is used. The term thunder day refers to the ground station hearing at least one auditory thunder clap in the observed day. This is a binary variable, with either a presence or no presence of thunder detected for each day. Fleagle (1949) concluded that the range of auditory thunder could rarely be heard beyond 24 km, while Brooks (1925) stated the range to be only 10-12 miles (approximately 16-19 km) under favorable conditions. Some factors that can influence the distance thunder can travel are thought to be temperature, density, eddies, gradients, humidity, topographical relief, and soil and vegetation type (Brooks, 1925; Changnon, 2001). No information is available for the time of detection, or the total number of thunder claps that were heard in each given day. According to NOAA, the station data collected after 1973 is much more reliable. For this study, only data occurring in 1975 and onward are used to ensure that only the most robust station data are incorporated for analysis. The raw data underwent rigorous automated quality assurance by NOAA, to interpret as much of the synoptic data as possible and to eliminate errors found in the raw data. Then, these data were quality controlled further in the creation of the summary of the day (https://www1.ncdc.noaa.gov/pub/data/gsod/readme. txt). A very small percentage of error may remain in the processed GSOD data set. After data processing, a total of 8,396 global stations are used for the analysis. It is known that certain influences such as altered localized noise, slight movement of stations, and urban influences impact the quality of detection of audible thunder (Changnon, 2001; Fleagle, 1949). These factors become less noticeable with the use of many stations. Studies in the past have discussed the influence of population density on the trends in severe weather such as tornados (Anderson et al., 2007; Brooks et al., 2003; Grazulis & Abbey, 1983; Schaefer & Galway, 1982). These studies concluded that human errors are the primary cause of spatial and temporal variability of tornado reports. While population density trends could possibly have a minimal influence on the auditory observations of thunder, only stations that were operational in 1975 and onward were used in the analysis, so there are no artificial trends in the number of stations present in each region. Tornado reports incorporate civilian accounts of tornado occurrence, which can strongly be biased by the increasing population around the world. However, thunder days are only reported by meteorological stations, which did not change in number throughout the four decades of analysis.

It is also important to note that the ground stations located in the country of China stopped recording the presence of thunder days after 2013. All thunder day calculations conducted in the region end in 2013 instead of 2017. In recent years, there have been transitions from human-observing weather stations to unmanned automatic weather stations, where thunder days are no longer reported. This transition is not unique to China and has been a cost-saving measure for an increasing number of regions of the world. A steep increase in the complexity and scope of automated weather sensors has been established in the last several decades (Merenti-Valimaki et al., 2001). This is noteworthy for thunder day observations, for which human observers are essential.

To ensure further that no artificial trends are observed in the data set, the occurrence of thunder days (%) is calculated for each station. Not every station observed the same number of days each year due to missing data, leap years, etc. To account for these discrepancies, the percent occurrence (%) is incorporated by using the summation of thunder days, divided by the summation of the total sampled days multiplied by 100 for each desired station or region in a particular year. The total sampled days were taken to be the total number of days for which any meteorological data were recorded for each station. The trends of the regional occurrence are then compared for the 43-year time period. Nine regions are selected for further thunder day occurrence analysis. These regions have been identified in previous literature as being convectively and electrically active regions of the world (Albrecht et al., 2016; Liu & Zipser, 2015; Zipser et al., 2006). The regions selected for thunder day analysis were SCUS, the Amazon, Argentina (Argen), Sahel, Congo, Maritime Continent, India/Himalayas (India/Hima), and Australia (Aust; black boxes in Figure 2). These nine regions are selected due to all showing some organized activity of thunder day trends, as well as being convectively active regions. The United States is selected due to the robust past literature on the electrical nature of the region. The regions are averaged over a relatively large area; therefore, the annual average number of thunder days reflects the nature of the larger region as a whole, instead of the smaller-scale areas that can produce a very large occurrence of annual thunder days. The selection of larger regions can reduce the number of expected annual thunder days in some regions such as India or Australia.



#### 2.2. Tropical Rainfall Measuring Mission Precipitation Features

This study uses 16 years of data from the Tropical Rainfall Measuring Mission (TRMM) satellite (1998–2013.) This satellite measures precipitation using a passive TRMM Microwave Imager, and the Ku-band precipitation radar (PR) in the latitude interval of approximately  $36^{\circ}N-36^{\circ}S$ . For this study, precipitation features (PFs) have been grouped together using the observations from the PR instrument. A PF is defined as contiguous raining pixels of greater than 75 km² observed by the TRMM PR that are grouped together to create a raining feature (Adhikari et al., 2018; Liu & Liu, 2016; Seto et al., 2013). The threshold of 75 km² was chosen because the contribution of total rainfall by PFs less than 75 km², based on the TRMM 2A25 algorithm, is less than 5% (Liu et al., 2010). Furthermore, the contribution to rainfall from PFs with an area of less than 75 km² and an echo top of greater than 4.5 km is less than 0.6%. Therefore, for ease of data processing, only larger PFs are included for the analysis.

For each PF observed during the 16-year period, the TRMM-LIS lightning flash count information is included with the feature. The TRMM-LIS is an optical lightning detection instrument mounted on the TRMM satellite (Christian et al., 1999). The satellite orbits at an altitude of approximately 360 km above the Earth's surface and 403 km after the orbit boost in August 2001. The field of view of the LIS is approximately 668 km at nadir, with a 4.3-km spatial resolution (Albrecht et al., 2011). After the boost of the satellite in August of 2001, the average view time of each pixel at nadir was approximately 92 s (Albrecht et al., 2011). Based on the flash locations, regional lightning flash density (flashes/km<sup>2</sup>/year) can be calculated. First, we calculate the summation of lightning flashes observed in the TRMM PF data set during the 16-year period in each gridded 5° × 5° box. Second, the summation of lightning flashes is divided by the area of the total sampled pixels in each  $5^{\circ} \times 5^{\circ}$  box, giving a value of flashes/km<sup>2</sup>. Third, the flashes per square kilometers are then divided by the average view time in seconds by the satellite of each 5° × 5° box, giving a flashes/ km<sup>2</sup>/s. Then we get the final flash density, with units of flashes/km<sup>2</sup>/year (Cecil et al., 2014), by multiplying by the number of seconds in a year. The number of lightning precipitation features (LPFs) was also calculated by determining the number of PFs with at least one flash of lightning in each  $5^{\circ} \times 5^{\circ}$  box. It is important to note that the TRMM pixel size and view time changed before and after the orbital boost. This was accounted for by calculating the area of each PF using the corresponding pixel size at the time of sampling, as well as the corresponding view time of each PF. Because the TRMM satellite is not in a Sun-synchronous orbit, it provides lightning flash observations in full diurnal cycle and also suffers from diurnal sampling biases. Negri et al. (2002) discussed the TRMM sample biases in the diurnal variation of precipitation and suggested that 3 years of data were needed to fully resolve the diurnal cycle of precipitation in a 12° grid. Though here we do not focus on the diurnal variation of lightning, the annual flash density on a  $5^{\circ} \times 5^{\circ}$  grid could suffer from a slight diurnal sampling biases. The Geostationary Lightning Mapper (GLM) on board the Geostationary Operational Environmental Satellite-R-East does not suffer this diurnal sampling bias (Rudlosky et al., 2019). This satellite, alongside other geostationary satellite missions in the future, will be valuable resources for monitoring lightning activity in real time with a more precise diurnal variability.

#### 2.3. Correlation Between the Ground Stations and the TRMM Lightning Parameters

To determine the significance of the correlation between the calculated variables (thunder days, flash density, and LPFs), a standard correlation coefficient (r value) was calculated for each  $5^{\circ} \times 5^{\circ}$  box. This value is always between -1 and 1, with positive values indicating positive linear correlations and negative values indicating negative or opposite correlation of the trends. The r values were calculated by creating a scatter of corresponding 16-yearly averaged thunder day occurrences, flash density, and number of LPFs in each box for the overlapping years. The r value was then calculated for the correlation of the scatter between the 16 points of each variable.

#### 3. Results

#### 3.1. Long-Term Interannual Variability of Global Thunder Day Occurrence

Utilizing 8,396 global ground-based meteorological stations, a global trend map of thunder day occurrence was created. The thunder day occurrence represents the percentage of total sampled days from each station that noted auditory thunder at least once in the monitored day. Figure 1a shows the 43-year (1975–2017) mean occurrence of thunder days at each station. Regions that exhibit a large occurrence of thunder day

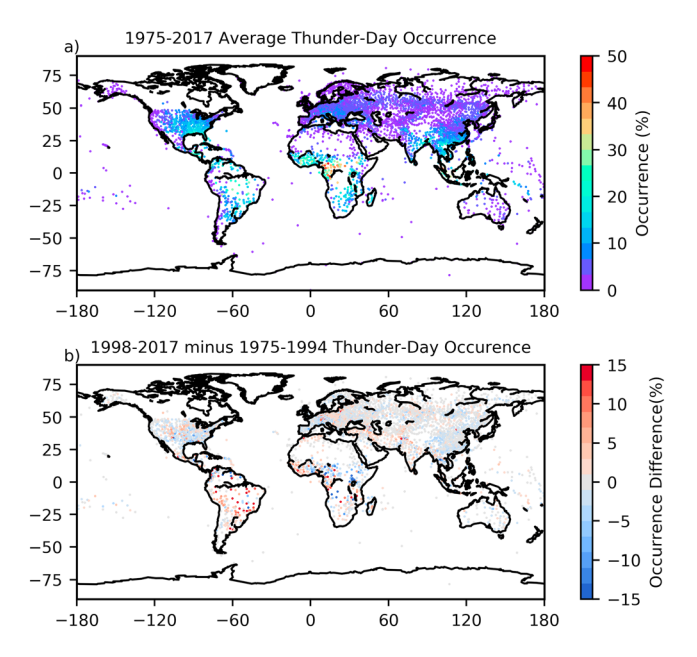


**Figure 1.** Difference in thunder day occurrence at ground stations between 1975–1994 and 1998–2017. Data are excluded after 2013 in China due to the lack of thunder day records. Thunder day occurrence is calculated using the summation of all the thunder days divided by the summation of all the total observation days in each region and presented as percentage.

activity include Central Africa, Southeast United States, Southeast Asia, Argentina, the Amazon, and Maritime Continent. Twenty-year mean occurrences were calculated for the first 20-year period (1975–1994), and the last 20-year data collection period (1998–2017). Twenty-year total occurrences were selected in order to make a more robust analysis, removing some of the interannual noise, such as uneven sampling or abnormal lightning activity. Figure 1b shows the difference for each ground station subtracting the final 20-year period from the first 20-year period, with warm colors indicating increasing thunder day occurrence and cool colors indicating decreasing thunder day occurrence. Clear regional trends can be observed throughout the globe, with regions such as China, India, Australia, the Amazon, and Western Europe showing clear thunder day tendencies during the study period.

China, which has a relatively robust ground station coverage (>500 stations), shows a decreasing trend in thunder day occurrence. This is consistent with the previous literature on trends in thunderstorms and hail in the region (Zhang et al., 2017). The most intense decrease in thunder day activity (5%–10%) can be seen in the southern portion of the country. The analysis reveals that the central portion of the region also observes significant decreases, and less of a trend is seen toward the northern and northeast regions of the country. Moving farther north into Russia, slight increasing trends in thunder day incidence is observed at a majority of the stations (<5%).

The sparse station coverage in the Amazon region displays the most intense and significant (10%–15%) increasing trend in thunder day occur-

rence in the world. A large increase in thunder days from the first 20-year period to the second is observed in the majority of the stations between  $0^{\circ}$  and  $-30^{\circ}$  latitude. The northern extremity of South America displays mixed trends, with no clear predominate shift in thunder day activity. The southern extremity of South America also shows systematic trends.

The United States, majority of Europe, and Africa display no clear consensus of trends on a station-by-station scale. In order to better understand the regional changes in thunder day occurrence, nine intense convective regions of the globe are selected. Figure 2 shows the nine selected regions, with each star representing a ground-based station within the region. The annual regional occurrence is calculated by taking the summation of all the thunder days heard inside each regional box and dividing by the total number of sampled days inside the regional box in each year and is summarized in Table 1. This value allows for a more robust analysis of the large-scale regional trends and removes the possible influences from regions with sparse station coverage. Table 1 summarizes the average number of thunder days observed in each convective region

annually as well as seasonally. A summary of the rate of annual and seasonal thunder day trends in each region during the sampled period is also shown in Table 1.

Figure 3 displays the yearly averaged trends in thunder day occurrence for each of the nine selected regions. During the 43-year period, six of the nine convectively intense regions display significant increasing trends in thunder day occurrence. As previously shown in Figure 1b, the Amazon region shows the largest increase, increasing from a 5% occurrence in the 1970s to 20% thunder day occurrence in the 2010s. This is an increase of approximately 13.3 thunder days per decade and is consistent with a previous study of Southeast Brazil, showing statistically significant increases in annual thunder days in this fast-developing and changing region of the world (Pinto et al., 2013). Also in South America, Argentina shows significant increases in thunder days (2.6 thunder days/decade). The region exhibits an increase from approximately an 8% occurrence in 1975 to

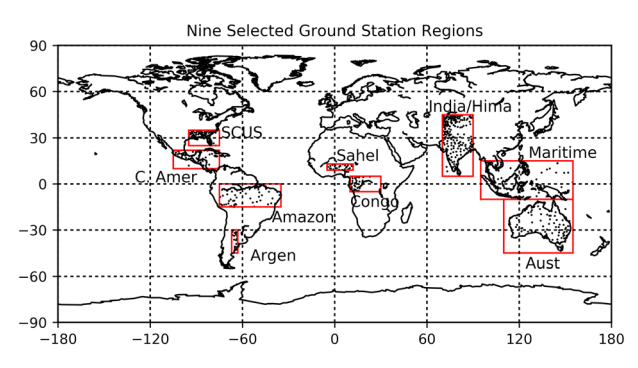


**Figure 2.** Nine selected convectively active regions. Each star represents a ground station. SCUS = South Central United States; Aust = Australia; C. Amer = Central America.



Table 1	
The 1975-2017 Annual and Seasonal Mean, and Annual and Seasonal	Trends in Thunder Days Over Nine Selected Regions

Time Period	Variation	Congo	Argen	India	Sahel	SCUS	Central America	Australia	Amazon	Maritime Continent
Annual	T day (day/year)	122.62	43.35	28.41	65.53	58.52	58.01	4.73	66.67	74.55
	Variation (day/decade)	6.9	2.6	2.0	-5.4	-0.9	4.7	-1.3	13.3	3.0
DJF	T day (day/year)	30.92	19.97	1.05	0.11	5.75	0.62	5.75	21.37	9.66
	Variation (day/decade)	1.7	1.2	0.1	-0.1	0.2	-0.1	-0.8	4.0	0.7
MAM	T day (day/year)	40.35	10.46	7.76	17.28	13.43	8.94	13.43	21.58	20.92
	Variation (day/decade)	2.3	0.5	0.7	-1.6	-0.4	0.5	-0.2	4.2	0.8
JJA	T day (day/year)	14.82	1.83	12.40	34.10	31.71	29.33	31.71	6.09	20.05
	Variation (day/decade)	0.8	0.02	0.6	-2.2	-0.1	2.4	-0.1	1.7	0.6
SON	T day (day/year)	36.61	11.18	7.20	13.49	6.68	18.85	6.68	17.73	20.89
	Variation (day/decade)	2.0	1.0	0.5	-1.5	-0.6	1.8	-0.4	3.4	0.9

Note. DJF = December-February; MAM = March-May; JJA = June-August; SON = September-November; SCUS = South Central United States.

11% in 2017, based on the slope of the trend line. Both large-scale intense lightning regions of South America (Amazonia and Argentina) are shown to have an increasing trend in thunder day occurrence.

The Congo region, one of the most intense convective regions of the world, exhibits an average of 123 thunder days per year in the large-scale region (Table 1). The central portion of the Congo region has very few stations available for analysis, and is underrepresented. However, the western portion of the Central Africa has a sufficient number of stations to build significant trends in the region. Figure 3a shows overall

#### 1975-2017 Regional Thunder-Day Trends

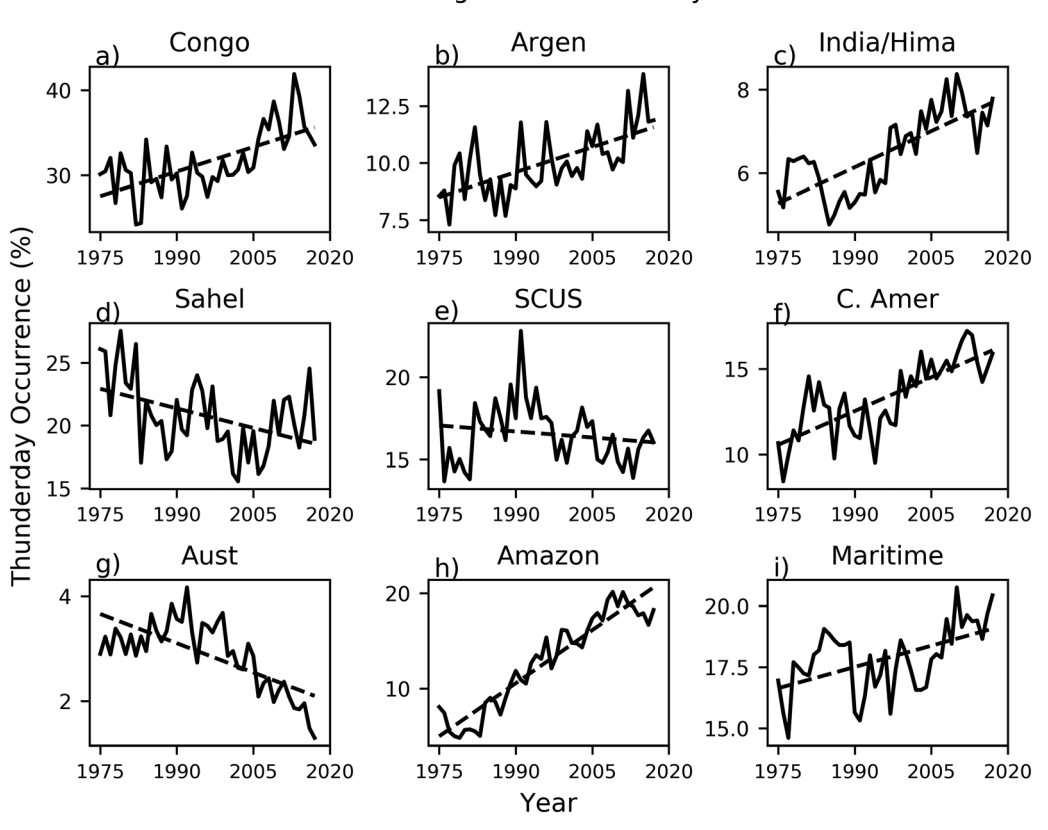


**Figure 3.** Trends in yearly thunder day occurrence in the nine selected global regions. Thunder day occurrence is calculated using the summation of all the thunder days divided by the summation of all the total observation days per year in each region and presented as percentage. SCUS = South Central United States; Aust = Australia; C. Amer = Central America.

increasing trends in the Congo region from approximately a 28% occurrence in the 1970s, to a 35% occurrence in the last several years, equating to an increase of 6.9 thunder days/decade. Smaller-scale processes appear to be influencing the thunder day trends in the continent of Africa as evidenced by Figure 3d, which demonstrates that the Sahel region exhibits opposite trends in thunder day activity in comparison to the Congo. Decreases in this region are observed from an approximate 24% occurrence to 17%, indicating a possible weakening in convective precipitation occurrence in the region with a decrease of 5.4 thunder days per decade.

Central America, the India/Himalayan, and the Maritime Continent regions all also exhibit significant increases in thunder day occurrence. Central America (Figure 3f) displays an increase in occurrence of approximately 11% to 15% over the course of the four decades, equating to an increase of 4.7 thunder days/decade. Figure 3c shows that the India/Himalayan region increases from 5% to 8%, and Figure 3i (Maritime Continent) shows the least intensification, shifting from 17% to 18%, equivalent to increases of 3 thunder days per decade.

Australia (Figure 3g) exhibits a decreasing trend in thunder days during the study period. The figure shows a shift from approximately a 4% to a 2% occurrence (-1.3 thunder day per decade) in the region. Figure 3e displays that the SCUS observes no clear trends (p value of 0.29) in thunder day activity, with the average occurrence in the region remaining at approximately 17%. All eight of the other convective regions show p values to be much less than 0.01, indicating a statistically significant change in thunder day frequency in the regions, although some of the trends are relatively weak such as Australia.

In order to understand some of the physical processes that possibly contribute to the trends exhibited in thunder days and flash density, a comparison is made with the results from the past literature on regional long-term thunder day trends. This comparison allows the results from Figures 1 and 3 to be supported or refuted.

In China, it is well documented that thunder day and thunderstorm activity has been decreasing since the 1950s (Zhang et al., 2017), which is corroborated with the results shown here. It has been shown that the reduction of thunder day events is strongly correlated with the weakening of the East Asian summer monsoon, which is the primary source of moisture and dynamic forcing conducive for warm season weather over China (Zhang et al., 2017). A weak correlation was also found between the cloud-to-ground flash density and number of lightning days in Guang-Dong Province, China (Chen et al., 2004). This weak correlation provides some evidence that the variation of cloud-to-cloud flashes may be more dominant in the relationship between flash density and thunder days in the region.

In the United States, Figures 3e and 5f show no significant changes in thunder day activity in the southcentral portion of the country annually or seasonally. This region was analyzed by Changnon (1985), stating that the variability of thunder days was correlated to cyclone frequency. A study conducted in the northern latitude of the country in Fairbanks, Alaska, revealed a 2 °C increase in summertime surface temperature from 1950 to 2005, accompanied by a simultaneous upward trend in number of annual thunder days (Williams, 1999). This indicates that thunderstorm activity in northern latitudes of the United States could be significantly influenced by the rise in global temperatures in the past 100 years. No significant large-scale trends are exhibited in Alaska as a whole in Figure 1b; however, several individual stations show increases in thunder day occurrence, especially in the northeast.

The increase in thunder day occurrence in Brazil in Figures 1b, 3h, and 3b can be tied primarily to the increase in urbanization of the region, and not to global warming. Compelling evidence was shown by Pinto (2015), stating that of the 14 cities that were studied, 12 had a large population increase since 1910. All of these 12 Brazilian cities that have since grown much larger also exhibited significant increases in thunder day occurrence. The other two cities (Rio de Janeiro and Cuiaba) were already large cities in 1910 and showed no significant growth in development or thunder days around the ground station sites. This provides evidence that the urban heat island effect, along with increased aerosols could be leading to a significant increase in thunder days in the large cities of this country (Pinto, 2015; Pinto et al., 2013).

The number of annual thunder days in the Siberian region has been detected to be decreasing by approximately 25% between 1966 and 1995 (Gorbatenko & Dulzon, 2001). This similar downward trend in thunder day occurrence is shown in Figure 1b in the far northeast of Siberia but is not clear throughout the entirety of

northern Russia. The downward trend in thunder days can be possibly attributed to shifting atmospheric circulation (Gorbatenko & Dulzon, 2001). A simultaneous downturn in cyclonic activity was observed during the study period, indicating that the suppression of these systems are leading to less thunderstorm activity. No trends in thunder day occurrence were observed in Germany during the years of 1974–2003 (Kunz et al., 2009). This is consistent with Figure 1b, which shows no significant trends in thunder days.

In the Northern Caucasus region, an increasing trend in thunderstorm activity was observed between 1936 and 2006 (Adzhiev & Adzhieva, 2009). This increase in annual thunder days is more pronounced over the high elevation and foothill areas of the region in Figure 1b. In this region, thunderstorm occurrence can be highly spatially variable, with just tens of kilometers of separation and a factor of 1.2–2 in thunder day occurrence. Figure 1b also shows the Northern Caucasus increasing from approximately a 4% to 6% annual occurrence of thunder days. However, the region just south of the Black and Caspian Seas, including Iraq and Iran, showed much larger increases in thunder days. This is consistent with past studies discussing increasing trends in annual thunder days in Iran (Araghi et al., 2016; Ghavidel et al., 2017). The region exhibits an increasing trend in thunder day occurrence between 1961 and 2010 in almost all months of the year, with April and May being the most significant (Araghi et al., 2016). This spring enhancement of this semiarid/arid region is hypothesized as being due to warming during the spring months, which are already the most humid of the year (Araghi et al., 2016). This could lead to more suitable conditions for thunderstorm activity.

#### 3.2. Long-Term Seasonal Variability of Global Thunder Day Occurrence

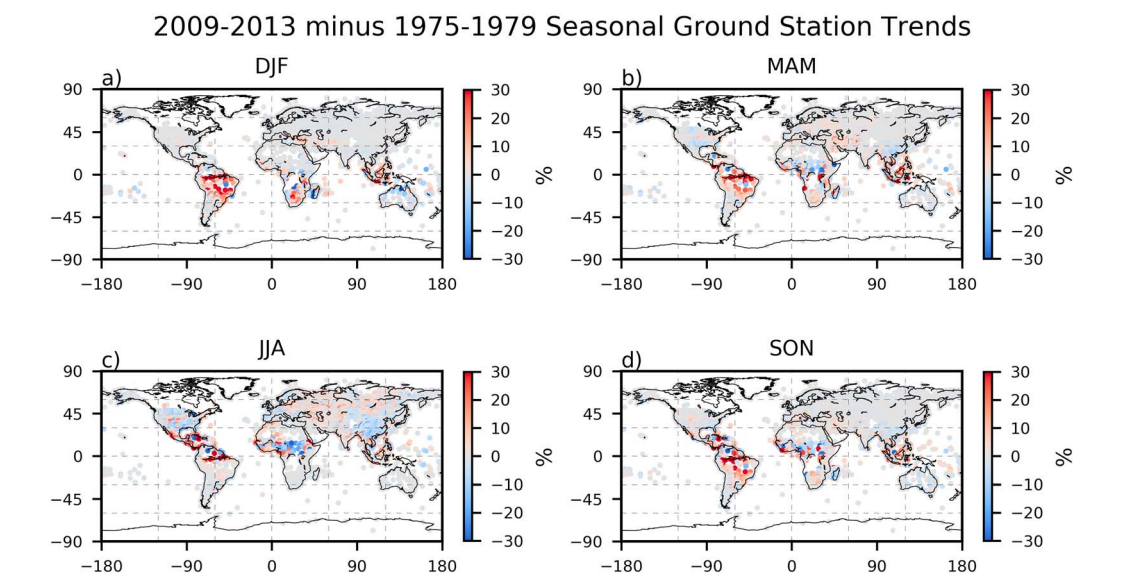
In order to observe a more detailed nature of trends in thunderstorms around the globe, a seasonal observation of thunder day trends has been conducted for each ground station. Figure 4 shows the global distribution of thunder day occurrence trend for each season: December–February (DJF), March–May (MAM), June–August (JJA), and September–November (SON). Figure 4a shows the trend of each station in the DJF season. The most noticeable trends in thunder day occurrence in this season occurs in the Southern Hemisphere. Most notably, Figure 4a shows increases in the majority of the South American region thunder day occurrence (25%–30%) from 1975–1984 to 2013–2017. Five-year periods were selected in order to minimize the interannual influence, and to obtain a more robust picture of the seasonal changes. The majority of stations in Southern Africa are also shown to have observed an increase in thunder days during the same time period. In contrast, Australia displays a decreasing trend in thunder days during their summer DJF season. Very little if any trends are noticed in the Northern Hemisphere during the DJF season. It should be noted that February is considered a severe weather month within the United States severe weather season and shows no significant trends in thunder days.

Figure 4b shows the trend in thunder days for the MAM season. The most notable trends on the station level in this season occurred in the Amazon, which exhibits an increase of approximately 10%–20%, and China which displays a decrease of approximately 10%–20% on average, which is consistent with the decreasing trends found in previous literature. (Zhang et al., 2017). Figure 4b also shows that the Maritime continent exhibits an increase in thunder day occurrence during MAM. No trends are found in the United States during the significant severe weather season of MAM.

Figure 4c displays the occurrence trends during the study period for the JJA season. Figure 4c shows that China exhibits a relatively large decrease in occurrence in this season (25%–30%). Most of Eastern Europe and Russia exhibit slight increases in thunder days during their summer season. The Maritime Continent and India also display significant increases during this season. It is important to note that during JJA, South America shows very little thunder day trends, while Africa appears mixed. The central portion of Africa exhibits decreasing trends, while the western portion shows primarily increasing trends. The southern portion of the continent exhibits very little trend in thunder day activity in JJA.

Figure 4d presents the seasonal trends during the SON season. Most notable increases in this season occur in the Amazon, Maritime Continent, and India. Noticeable decreases can be observed in the figure in China and Australia during SON as well.

In order to determine the seasonal ground station trends for the convectively active regions of the globe, the same nine regions were used for the seasonal analysis. Figure 5 shows this results. Figure 5 shows that each region displays a unique pattern of thunder day trend activity. Several regions such as the Maritime



# **Figure 4.** Seasonal trends in global thunder day occurrence observed by the ground stations. Thunder day occurrence is calculated using the summation of all the thunder days divided by the summation of all the total observation days in each region and presented as percentage. Five-year averages were selected to reduce the impact of interannual variability such as a strong Mesoscale Convective System event. DJF = December–February; MAM = March–May; JJA = June–August; SON = September–November.

1975-2017 Seasonal Ground Station Trends

#### India/Hima Congo MAM SON DJF SCUS Sahel C. America Occurence (%) Maritime Australia Amazon h) Year

**Figure 5.** Seasonal trends in thunder day occurrence in the nine selected regions. SCUS = South Central United States; Aust = Australia; C. Amer = Central America; DJF = December–February; MAM = March–May; JJA = June–August; SON = September–November.

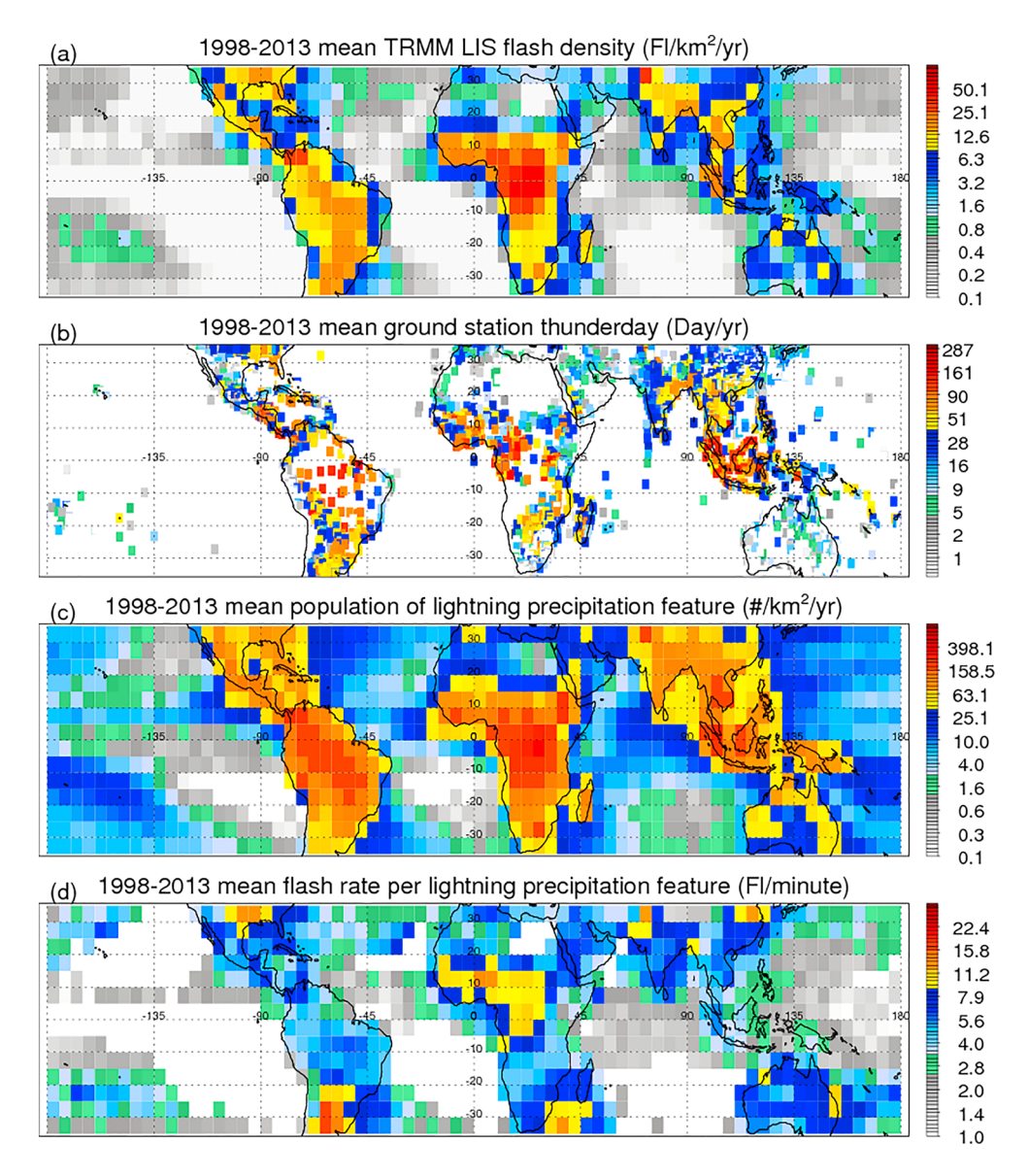


**Figure 6.** (a) Mean Tropical Rainfall Measuring Mission-Lightning Imaging Sensor (TRMM-LIS) flash density in 1998–2013 presented as flashes/km<sup>2</sup>/year over  $5^{\circ} \times 5^{\circ}$  grids. (b) Mean thunder day reports per year from ground stations during the TRMM era, (c) the mean population of lightning precipitation features (PFs; #/km<sup>2</sup>/year), and (d) the average flash rate per lightning PF (flash/min/PF). All variables are averaged in  $5^{\circ} \times 5^{\circ}$  bins.

Continent and the Amazon also exhibit a relatively large occurrence in the local spring and fall months. Figure 5 strengthens the idea that global and regional trends in thunderstorm activity can be monitored seasonally, with certain regions of the globe showing increases or decreases in thunder day occurrence. This is important to be able to refine the temporal scales in which the trends occur, in order to determine how the changing climate influences regional thunderstorm activity in more detail.

#### 3.3. Comparison of Ground Station Thunder Days to TRMM-LIS Flash Density

Figure 6 shows the comparison of the three 16-year (1998–2013) averaged TRMM-LIS variables: flash density (Figure 6a), population of LPFs (Figure 6c), and flash rate (Figure 6d), to the mean annual thunder days per year calculated during the same 16-year period (Figure 6b). The thunder day, flash density, and population of LPFs are largely in agreement in spatial distribution. Figure 6a, showing the flash density binned in  $5^{\circ} \times 5^{\circ}$  boxes, reveals relatively high flash density in Central Africa, South America, southern United States, eastern India, and the western Maritime Continent. This is consistent with past satellite-based



observations of lightning density (Albrecht et al., 2016; Cecil et al., 2014; Christian et al., 2003; Rudlosky et al., 2019). The thunder day frequency shown in Figure 6b displays positive qualitative spatial agreement with the flash density observed by TRMM. The regions of the world with the highest frequency of annual thunder days are shown to be Central Africa, Amazon, Argentina, southeast United States, eastern India, Southeast Asia, and the Maritime Continent. It appears that certain regions such as the Maritime Continent and the Amazon have a larger number of annual thunder days to flash density ratio than most of the world. This provides evidence that these regions see a relatively large number of thunderstorms that produce relatively few lightning strikes per event, which is consistent with the literature (Cecil et al., 2015). This is supported by Figure 6a, which shows that the Amazon, Central Africa, and the Maritime Continent produce the largest number of flashes/km²/year over large regions. Overall, the 16-year averaged annual thunder days shows positive spatial correlation to the TRMM flash density.

#### 3.4. Comparison of Thunder Day and TRMM-LIS Flash Trends

In order to take a more comprehensive approach to observing the global shifts and trends in lightning activity, this study applies the use of multiple independent data sources. It is important to understand the agreement/disagreement between the trends in thunder days observed by the ground stations, and the trends in flash density and population of LPFs observed by the TRMM satellite. Recognizing these agreements/disagreements can allow us to better verify the shifting in electrical nature of storms around the globe, as well as learn about some of the properties of the precipitation systems that are occurring. Although 16 years of the LIS data is not a long enough time span to deduce robust climatological trends, it is one of the longest and most trusted set of global satellite lightning flash data that is available to date. Figure 7 compares the two data sources, both averaged in  $5^{\circ} \times 5^{\circ}$  boxes. Figure 7a shows the flash density change in each 5° × 5° box. Figure 7b shows the interpolated ground station thunder day change during 1998-2013. Increasing trends in the mean number of days exhibiting auditory thunder occur in the Amazon, Central America, Western Africa, the Middle East, India, and the Maritime Continent. Fewer observed thunder days are shown in Australia, China, northcentral Africa, and Argentina. Figure 7c displays the trend in annual number of LPFs ( $\#/\text{km}^2/\text{year}$ ) in each 5° × 5° box. Similar qualitative spatial patterns are observed in this variable as are seen in the thunder day trends (Figure 7b), with increasing number of thunderstorms annually occurring in Western Africa, the Middle East, Southern India, and the Maritime Continent. Regions with a declining number of annual thunderstorms include; Australia, South Africa, China, and western North America.

Figure 7d investigates the correlation between the trend in flash density and the trend in thunder day frequency in each  $5^{\circ} \times 5^{\circ}$  box. The results show that the correlation between the two variables vary regionally; however, most of the TRMM domain shows a positive correlation (r value). These regions of positive correlation include China, Australia, the Maritime Continent, the Middle East, South Africa, Argentina, and Central America. A few regions show an opposite trend in thunder day occurrence and flash density. These include Southeast Asia, northcentral Africa, and Western Africa. This result indicates that although there is a positive agreement over much of the tropics and subtropics, the thunder day and flash density variables are not always directly correlated. To further investigate the relationship between thunder days and TRMM-LIS parameters, the trend in thunder day occurrence (Figure 7b) was compared to the trend in number of annual LPFs (Figure 7c) in each 5° × 5° box. Figure 7e shows the correlation coefficient for each bin. The results show an even higher correlation between the trend in thunder days and the trend in number of LPFs, with the majority of the TRMM domain, showing a positive relationship between the two variables. Many regions such as South Africa, China, the Maritime Continent, Central America, Argentina, and the Middle East show r values of greater than 0.6. Having such a positively correlated interannual agreement between these two variables, which are measured using two completely different data sets, provides enhanced evidence that the trends observed are indeed trustworthy.

To understand why the trend in thunder days and the trend in flash density are so highly correlated in some regions, and not at all correlated in others, four highly correlated and four uncorrelated regions were chosen for further investigation. The regions are shown as the boxes in Figure 7. It is important to note that these regions are not the same as selected in Figure 2, which focuses on regions with more obvious trends. Figure 8 shows the 16-year time series of the thunder day occurrence (solid black), flash density (dashed), number of LPFs (dotted), and the flash rate/PF (blue) for the four correlated regions. All of these regions

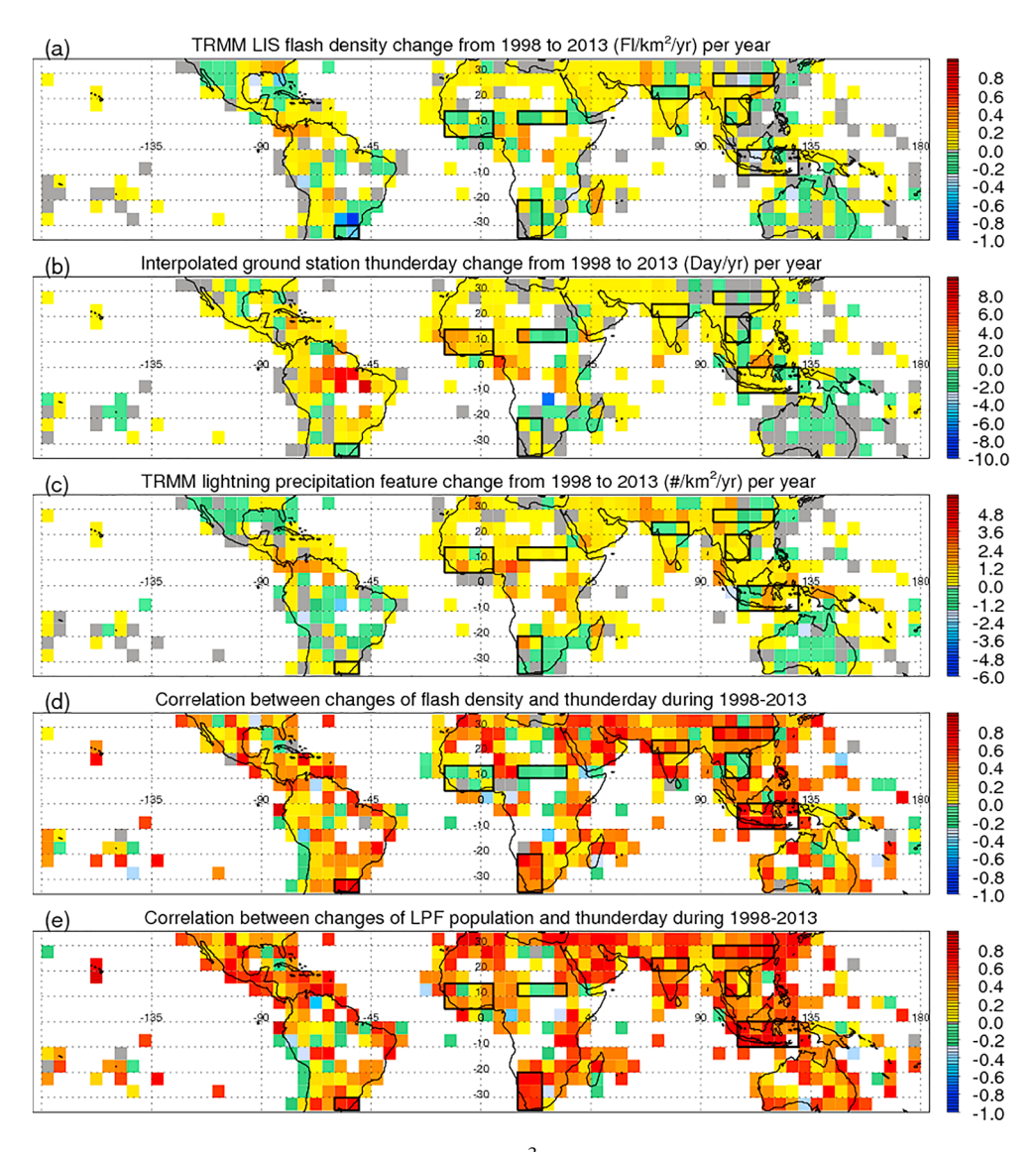


**Figure 7.** (a) The trend in lightning flash density (flash/km $^2$ ) as observed by the Tropical Rainfall Measuring Mission (TRMM) satellite. (b) The interpolated ground station thunder day trend between 1998 and 2013, (c) the trend in number of lightning precipitation features (observed) by the TRMM satellite. (d) The correlation between panels (a) and (b) for each  $5^{\circ} \times 5^{\circ}$  bin. (e) The correlation between panels (b) and (c) for each  $5^{\circ} \times 5^{\circ}$  bin.

show positive correlation coefficients of at least 0.58, with the Maritime Continent, China, and Argentina all showing correlation coefficients of above 0.8 between the flash density and thunder day variables. For these four regions, the interannual variability of the thunder day occurrence, flash density, and number of lightning PFs all show positive linear agreement over the 16 years. Interestingly, the flash rate/PF (flashes/min/PF) variable also exhibit a positive relationship to the other three variables in all four highly correlated regions. In these regions, the number of thunderstorms and the number of flashes/thunderstorm are at least slightly positively correlated.

In contrast, Figure 9 shows the four uncorrelated regions between the thunder days and flash density. In these regions the flash density is more correlated to the flash rate/LPF, with all correlation coefficients of at least 0.66, than the total number of LPFs. This indicates that in these regions, the flash density is strongly driven by the amount of flashes in each thunderstorm. In all four uncorrelated regions in Figure 9, the number of LPFs and the flash rate/LPF are negatively or poorly correlated. For example, in these regions, if the number of annual thunderstorms is increasing, the flash rate/thunderstorm is either decreasing or showing no correlation to the number of thunderstorms, and vice versa. Table 2 displays the correlation coefficients of

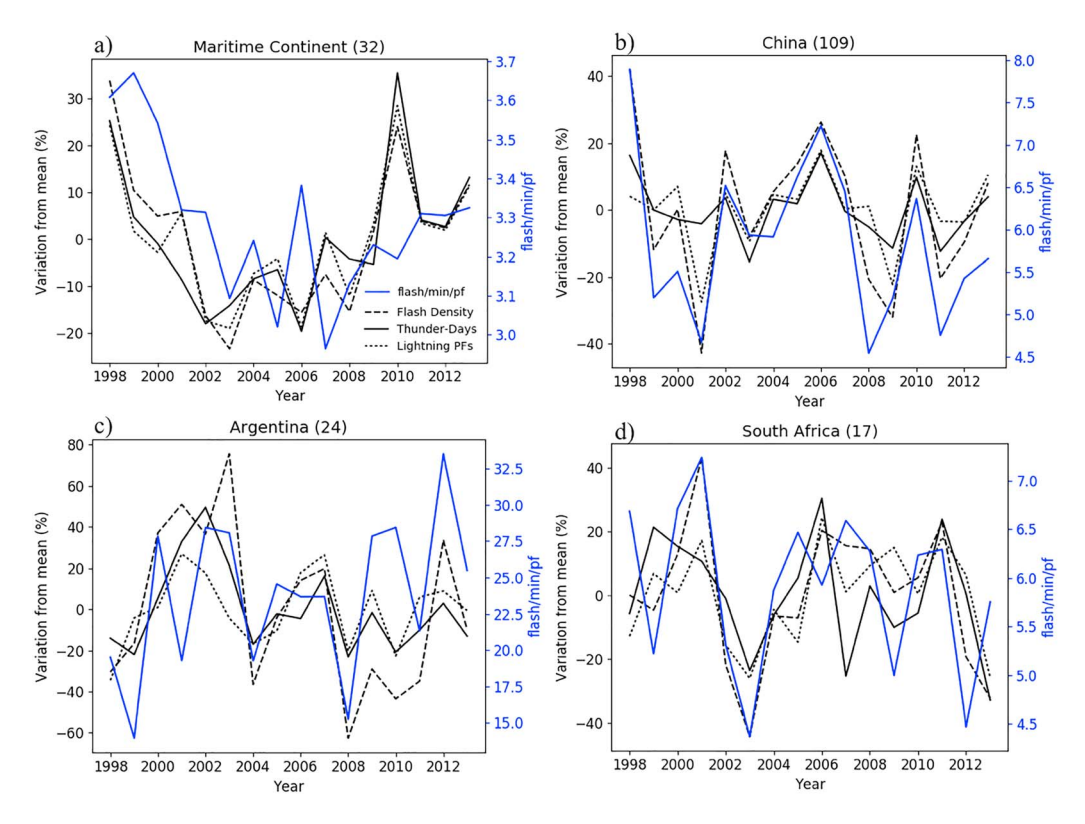


**Figure 8.** Time series of the number of annual thunder days (solid), lightning flash density (dashed), number of lightning precipitation features (LPF; dotted), and number of flashes/minute/LPF (blue), observed in the Tropical Rainfall Measuring Mission domain (1998–2013) for four regions showing good agreement between thunder days and lightning flash density. Flash density, thunder days, and LPF are expressed as a percent deviation from their 16-year mean (%). The number in parentheses indicates the number of ground stations in the region.

the regional lightning variables for all eight of the selected regions. In all cases, if the flash rate is uncorrelated to the number of LPFs, the thunder day to flash density correlation is also poor. However, if the correlation between the flash rate/LPF and number of LPFs is at least slightly positive, the correlation between the thunder day occurrence and the flash density is significant (r value >0.58). This indicates that regions that show a positive correlation between the flash rate and number of LPFs also show a similar trend in flash density and thunder day occurrence. This is important because of the relatively longer time series of thunder day data, extending much further than the satellite era (some stations date back to 1930). Understanding how we can utilize the combination of thunder day and satellite flashcount data to better reveal the global and regional trends in lightning flash density in the past four decades and beyond is valuable to better distinguish the past tendencies in thunderstorm activity. Although we do not have satellite measured lightning flash density prior to the late 1900s, the similarities in interannual variability between thunder day occurrence and flash density in some specific regions allows us to possibly estimate the past lightning activity over a longer period of time. Figure 10 shows the 43-year time series of thunder days occurrence (solid), flash density (dashed), and number of lightning PFs (dotted) for three selected regions (Southern Maritime Continent, Middle East, and China). The interannual agreement between the three variables during the TRMM era adds confidence in the longer thunder day data set in these regions, to observe the trends in lightning activity over the past four decades. In the Southern Maritime Continent (Figure 10a), and the Middle East (Figure 10b), slight but significant (p value <0.1) increases in lightning activity can be inferred. In China (Figure 10c), a significant decrease in lightning activity was observed since 1975 (p value <0.01), which is corroborated with the literature (Zhang et al., 2017). With this ability to use the combination of the ground station thunder day data, and the new age lightning observations from space to infer regional lightning activity trends over a much longer timespan, gives us a unique opportunity to possibly study the impact of climate change on the electrical nature of storms around the globe.

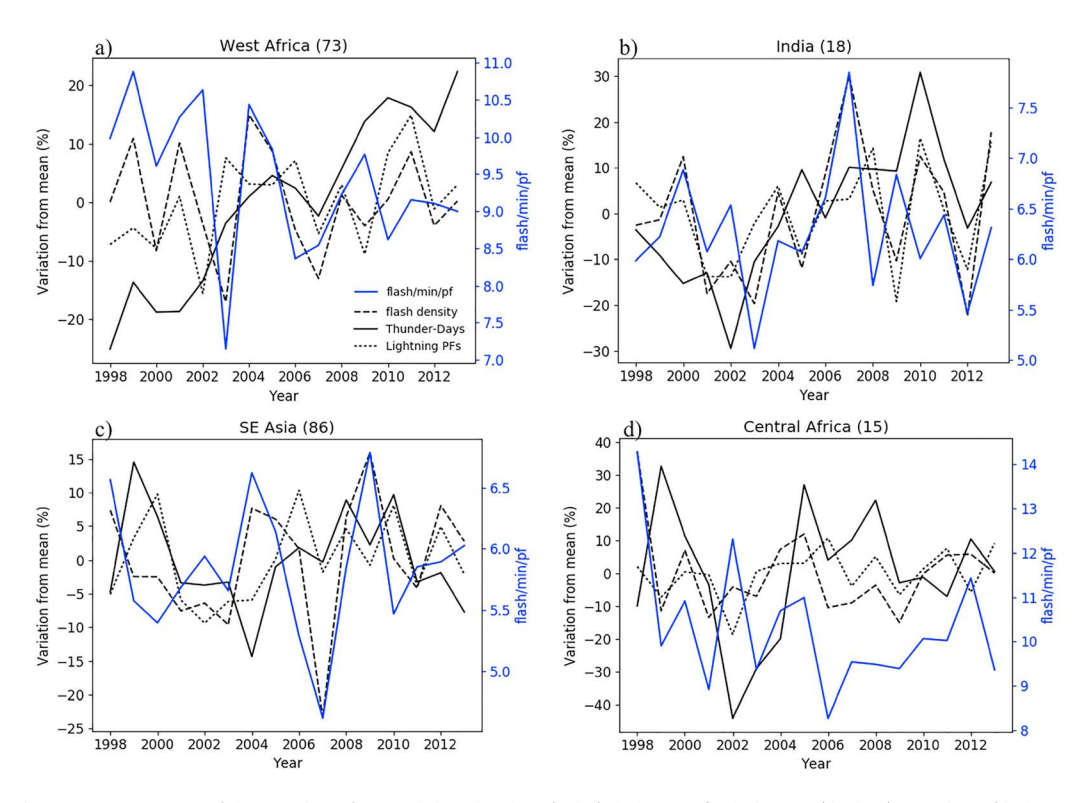


**Figure 9.** Time series of the number of annual thunder days (solid), lightning flash density (dashed), number of lightning precipitation feature (LPF; dotted), and number of flashes/minute/LPF (blue), observed in the Tropical Rainfall Measuring Mission domain (1998–2013) for four regions showing poor agreement between thunder days and lightning flash density. Flash density, thunder days, and LPF are expressed as a percent deviation from their 16-year mean (%). The number in parentheses indicates the number of ground stations in the region.

#### 4. Discussion

#### 4.1. Annual and Seasonal Trends in Thunder Day Occurrence Around the Globe

The global map of the 8,360 ground-based stations shown in Figure 1a provides evidence as to how the electrical nature of thunderstorms has changed over the past four decades. Figure 1b indicates that regional forcing is influential in determining the pattern of thunder day activity, as no true global consensus is observed. However, it is should be noted that six of the nine selected convectively active regions show significant increases in thunder day occurrence, providing evidence that thunderstorm activity is possibly increasing in the tropics with a warming climate. This differs from analysis from Finney et al. (2018), stating that a decrease in global lightning may be observed over the course of the next century, using a new ice flux parameterization. These regional shifts, shown in Figure 3, are largely corroborated by the past literature

**Table 2**Correlation of Regional Lightning Variables (r Values): Thunder Day (TD), Flash Density (FD), Flash Rate (FR), and Lightning Precipitation Features (LPFs) 1998–2013

Region	TD-FR	FD-FR	TD-LPF	FD-LPF	LPF-FR	TD-FD
Maritime Continent	0.23	0.56	0.93	0.94	0.25	0.88
China	0.76	0.92	0.69	0.81	0.55	0.81
Argentina	0.40	0.47	0.68	0.60	0.26	0.81
South Africa	0.24	0.75	0.69	0.80	0.22	0.58
West Africa	-0.41	0.69	0.55	0.23	-0.53	0.03
North India	0.07	0.66	0.46	0.71	-0.04	0.43
Southeast Asia	-0.42	0.81	0.68	0.21	-0.40	-0.04
Central Africa	-0.25	0.83	0.28	0.23	-0.36	-0.05

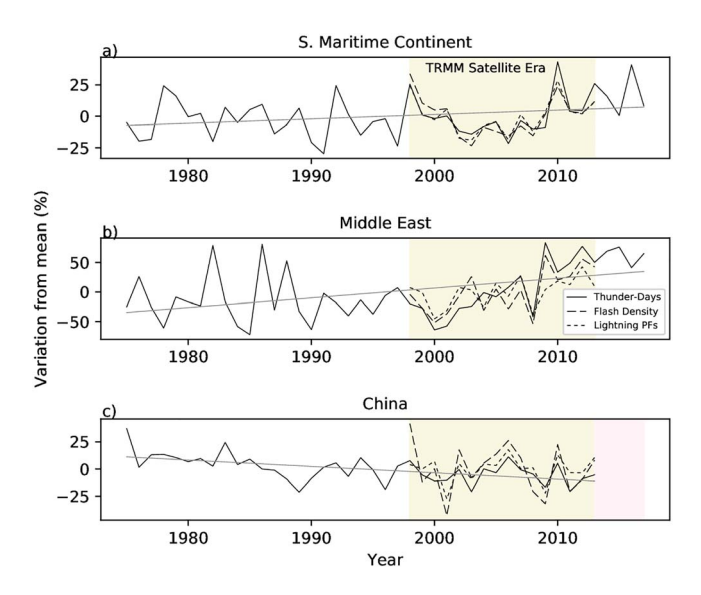


**Figure 10.** Time series of thunder days (solid), lightning flash density (dashed), and number of lightning precipitation features (PFs; dotted) for three regions. The tan region shows the time period of the Tropical Rainfall Measuring Mission (TRMM) satellite era. No thunder day data are available for the China region after 2013 represented in light red.

conducted around the world, providing further evidence to the validity of the trends. For example, deep convection in China is possibly being suppressed by the weakening Summer Asian Monsoon, with the anomaly in the summer monsoon index decreasing sharply from 1965 to 2005 (Zhang et al., 2017). This result is verified by the GSOD ground station decrease in thunder day occurrence. The past four decades of ground station results also verify the past literature observed in Europe. A European divide is displayed in thunder day trends, with the western portion of Europe, including the Baltic observing primarily decreasing trends in thunder days. The Eastern portion of Europe, incorporating Eurasia, exhibits predominately increasing trends in thunder day activity. This is possibly caused by the increasing Convective Available Potential Energy and moisture in the east, which enhances thunderstorm activity, and the increase in number of northerly circulation type weather events in the west, which suppresses thunderstorm activity (Enno et al., 2014; Ye et al., 2017). In the Amazon, the long-term behavior of GSOD ground stations support previous studies of upward trending lightning activity in the region Pinto et al. (2013).

Understanding how these regions are shifting in thunder day occurrence seasonally is important to understand the temporal scales in which the global aggregate of lightning activity is also changing. For example, with the intense increase in thunder day occurrence in South America, it is rea-

sonable to expect a relatively larger proportion of lightning activity occurring during the convectively active periods (i.e., DJF and SON) than that occurred 43 years ago. Likewise, evidence suggests that the period of convective activity over the continent of Australia (DJF) could see less contribution to global lightning and electrified cloud activity than it did previously. Monitoring these shifts to the seasonal and interannual variability of total global lightning and electrified cloud parameters such as area of 30 dBZ in the mixed phase temperature region, which has been shown with a high correlation with global electric circuit (Lavigne et al., 2017), could be a useful technique in monitoring the trends in regional lightning activity in a changing climate.

#### 4.2. Trends Observed by the TRMM-LIS Instrument

Figure 7a shows the 16-year average trend in lightning flash density for each 5° × 5° box. Many tropical and subtropical regions observe at least slight increases in lightning flash density over from 1998 to 2013, including Southern India, Southeast Asia, the Maritime Continent, the Middle East, and Central America. This is consistent with the theory that in a warming climate, increased lightning in the tropics and subtropics should be observed (Price & Rind, 1994; Reeve & Toumi, 1999; Williams, 1992, 1994, 1999). However, some regions such as Australia, China, and South Africa appear to have decreasing trends in flash density in the past 16 years. This indicates that other localized effects may play a role in some regions of the world. It is important to note the role of MCS on the observed trends in interannual variability of thunderstorm activity in certain regions. Goodman and MacGorman (1986) described that in the United States, a single intense MCS event can contribute 25% of the total annual lightning flashes. It is possible that only a few of these intense MCS events could bias the interannual variability and lead to significant climatological trends. The thunder day record of intense MCS events does not reflect the many thousands of flashes in the given day. However, these large systems are typically reported by numerous ground stations, possibly accounting for some of the bias. ENSO events have also been shown to influence regional lightning patterns (Goodman et al., 2000). For example, the warm ENSO phase has been associated with an increase in lightning activity over the western Maritime Continent (Chronis et al., 2008; Hamid et al., 2001). This also indicates that ENSO related phases can influence the interannual climatology of lightning and must be accounted for when discussing trends in regional lightning frequency. More work is needed in the future to determine the largescale versus localized influences to lightning activity trends around the globe. As more flash count data becomes available in the future, a clearer picture of regional lightning trends via satellite can possibly be drawn (Blakeslee et al., 2014; Goodman et al., 2013).



#### 4.3. Comparison of Ground Station Trends to TRMM-LIS Trends

Figure 6 shows that the spatial distribution of annual thunder days and annual flash density is largely consistent with each other over a 16-year period. Several regions such as the Amazon and Maritime Continent exhibit disproportional ratios of thunder days to flash density relative to other regional observations. These unique regions exhibit a large number of LPFs, with a relatively lower number of flashes per LPF. The flash density is dominated by the large number of LPFs, rather than the intensity of the thunderstorms. However, the majority of the rest of the tropics and subtropics are in agreement on the spatial distribution of annual thunder days and annual flash density. This allows for the next logical step to discern whether or not the relatively longer-term trends in these variables is also consistent with each other. It is important to note that 16 years of observations is not ideal for understanding long-term trends in lightning activity. It is, however, reasonable and advantageous to look at the agreement/disagreement between the thunder day trends and flash density trends during the same period of time to understand if any new information can be drawn. Figure 7d shows that many regions in the tropics and subtropics are in agreement (positive linear relationship), such as Australia, the Maritime Continent, Argentina, China, Central America, the Middle East, and South Africa. This provides some evidence that the satellite trends are verified by ground-based observations of thunder days, and vice versa. Figure 7e provides more evidence for this, showing that the correlation between thunder day occurrence and number of TRMM LPFs is even more highly correlated than the flash density. Almost all regions of the tropics and subtropics are in positive linear agreement between the trends in thunder days and trends in number of LPFs. This indicates that the interannual variability of thunder days is more correlated to the number of thunderstorms than the number of total flashes.

There are some regional cases, however, in which the satellite trends are not verified by the ground station measurements. Most notable of these areas are western Africa, northcentral Africa, Southeast Asia, and northern India. This disagreement led to an interesting finding in that in all of the poorly correlated regions (Figure 9), opposite or no correlation of the trends in number of thunderstorms and flashes/thunderstorm is observed. For example, Northern India observes an increase in annual thunder days during the TRMM domain, but a subsequent decrease in lightning flash density. This disagreement can be explained by the fact that the region observes an increasing trend in number of annual thunderstorms, but a decreasing trend in flashes/thunderstorm, which indicates that the thunderstorms are becoming weaker. This led to the observation of more numerous thunder days, but fewer total lightning strikes.

This finding is important because it illustrates the idea that trends in thunder days and trends in flash density are not always correlated. An increase in occurrence of thunder days over some regions cannot lead to the direct assumption that the total number of lightning flashes will also increase. More work is needed in the future to verify these claims, but it is important to point out the regions of agreement/disagreement in thunder day/flash density trends over the past 16 years.

#### 5. Summary

This study aimed to utilize over 8,000 ground-based stations over the course of 43 years, in order to determine global trends in thunder day occurrence for the purpose of understanding how the global aggregate lightning activity has been shifting since the Industrial Revolution. These thunder day trends were also compared to the simultaneous trends in flash density, and number of thunderstorms observed by the TRMM satellite, in order to verify or counter the regional trends observed by the ground stations. The major findings include the following:

- Clear regional trends are observed by the ground station during the past four decades in yearly thunder day occurrence. Regions such as the Amazon, Maritime Continent, India, the Himalayas, Central America, Argentina, and the Congo all observe increases in thunder day occurrence. In contrast, regions such as China, Australia, the Sahel, and parts of Western Europe all display decreases in thunder day occurrence. It is important to emphasize the significance that the majority of the selected regions exhibited significant increases in thunder day activity in the past four decades.
- 2. Seasonal trends are also observed globally in thunder day activity, with each season resulting in unique tendencies in regional thunder day occurrence. Primarily, the largest occurrence and steepest trends in annual thunder days occur in the local summer season. The Maritime Continent and Amazon region exhibit a unique three-season active thunder day period, with only the local winter season exhibiting a



- low occurrence. Of the nine sampled regions, only the SCUS does not show any statistically significant trends in thunder days in any season. All the other eight regions display significant (p value <0.05) for at least certain seasons, resulting in a changing seasonal as well as annual local climatology in thunder-storm activity.
- 3. Regional spatial agreement is present between the trends observed in the ground station thunder days and the satellite flash density, as well as annual number of LPFs. This provides evidence that the two independent data collection methods are corroborating each other. Regions such as the Maritime Continent, China, South Africa, and Argentina show strong positive correlation (*r* value >0.58) between the trends in the thunder day and flash density variables. These regions show an even larger correlation (>0.68) between the trends in thunder days and number of annual LPFs. All of these regions have at least a slight positive correlation between the trend in number of annual thunderstorms and the trend in the flash rate/thunderstorm. Other regions, for which there is disagreement on the relationship between trends in thunder days and the flash density, all have negative or no correlation between the number of thunderstorms and the number of flashes/LPF.

The regional agreement between the ground stations and the satellite trends of several global regions that favor lightning activity provides supporting evidence that satellites can be helpful in the future in monitoring global lightning shifts. As more data become available from the International Space Station-Lightning Imaging Sensor, as well as geostationary satellites, such as the Geostationary Operational Environmental Satellite-R Series Global Lightning Mapper, we can continue to improve on determining the impact of climate change on lightning activity. The regions of disagreement, such as northern India, allow for interesting case studies into the region, showing that possible shifts in system type are occurring. For the case of northern India, the disagreement in flash density and thunder day occurrence indicates significant evidence that the area is receiving more thunderstorms that are relatively weaker and produce less lightning.

Ultimately, an insufficiently long satellite data set is available to make any definite claims as to the trends in lightning flash density as it pertains to the changing climate. However, the combination of the satellite data, alongside longer-term ground station data, provides evidence that many regions are observing shifts in lightning activity at the interannual, annual, and seasonal timescales. Monitoring this global aggregated joint seasonal-diurnal shift in lightning and other electrified parameters can possibly be useful in the future in monitoring the changing climate. It is becoming clear that the relatively longer temporal span of lightning data from space is allowing for satellite technology to become more useful to determine the long-term variability of atmospheric electricity. By utilizing the past satellite record, alongside the newer satellite instruments such as International Space Station-Lightning Imaging Sensor and GLM, we can understand with more confidence the variability of lightning and thunderstorms at various temporal time scales.

#### Acknowledgments

Thanks to Earle Williams, Steven Goodman, and an anonymous reviewer for valuable suggestions. This study was supported by NSF-1519006 and NASA PMM science NNXAD76G. Thanks to Erich Stocker and the Precipitation Processing System (PPS) team at NASA Goddard Space Flight Center, Greenbelt, MD, for TRMM data processing assistance. This TRMM data can be downloaded from http://atmos.tamucc.edu/trmm/data/. The GSOD ground station data can be downloaded from https://data.nodc.noaa.gov/cgibin/iso?id=gov.noaa.ncdc:C00516.

#### References

Adhikari, A., Liu, C., & Kulie, M. S. (2018). Global distribution of snow precipitation features and their properties from 3 years of GPM observations. *Journal of Climate*, 31(10), 3731–3754. https://doi.org/10.1175/JCLI-D-17-0012.1

Adlerman, E. J., & Williams, E. R. (1996). Seasonal variation of the global electrical circuit. *Journal of Geophysical Research*, 101(D23), 29,679–29,688. https://doi.org/10.1029/96JD01547

Adzhiev, A. K., & Adzhieva, A. A. (2009). Spatial and temporal variations of thunderstorm activity in the Northern Caucasus. *Russian Meteorology and Hydrology*, 34(12), 789–793. https://doi.org/10.3103/S1068373909120036

Aich, V., Holzworth, R. H., Goodman, S. J., Kuleshov, Y., Price, C., & Williams, E. R. (2018). Lightning: A new essential climate variable. Eos, 99. https://doi.org/10.1029/2018EO104583

Albrecht, R. I., Goodman, S. J., Buechler, D. E., Blakeslee, R. J., & Christian, H. J. (2016). Where are the lightning hotspots on earth? *Bulletin of the American Meteorological Society*, 97(11), 2051–2068. https://doi.org/10.1175/BAMS-D-14-00193.1

Albrecht, R. I., Goodman, S. J., Petersen, W. A., Buechler, D. E., Bruning, E. C., Blakeslee, R. J., & Christian, H. J. (2011). The 13 years of TRMM lightning imaging sensor: From individual flash characteristics to decadal tendencies, XIV International Conference on Atmospheric Electricity, August 08–12, 2011, Rio de Janeiro, Brazil.

Anderson, C. J., Wikle, C. K., Zhou, Q., & Royle, J. A. (2007). Population influences on tornado reports in the United States. Weather and Forecasting, 22(3), 571–579. https://doi.org/10.1175/WAF997.1

Araghi, A., Adamowski, J., & Jaghargh, M. R. (2016). Detection of trends in days with thunderstorms in Iran over the past five decades. Atmospheric Research, 172, 174–185.

Blakeslee, R. J., Mach, D. M., Bateman, M. G., & Bailey, J. C. (2014). Seasonal variations in the lightning diurnal cycle and implications for the global electric circuit. *Atmospheric Research*, 135, 228–243.

Brooks, C. E. P. (1925). The distribution of thunderstorms over the globe. Geophysical Memoirs London, 24, 147-164.

Brooks, H. E., Lee, J. W., & Craven, J. P. (2003). The spatial distribution of severe thunderstorm and tornado environments from global reanalysis data. *Atmospheric Research*, 67–68, 73–94.



- Cecil, D. J., Buechler, D. E., & Blakeslee, R. J. (2014). Gridded lightning climatology from TRMM-LIS and OTD: Dataset description. Atmospheric Research, 135, 404–414.
- Cecil, D. J., Buechler, D. E., & Blakeslee, R. J. (2015). TRMM LIS climatology of thunderstorm occurrence and conditional lightning flash rates. Journal of Climate, 28(16), 6536–6547. https://doi.org/10.1175/JCLI-D-15-0124.1
- Cecil, D. J., Goodman, S. J., Boccippio, D. J., Zipser, E. J., & Nesbitt, S. W. (2005). Three years of TRMM precipitation features. Part I: Radar, radiometric, and lightning characteristics. *Monthly Weather Review*, 133(3), 543–566. https://doi.org/10.1175/MWR-2876.1
- Changnon, S. A. (1985). Secular variations in thunder-day frequencies in the twentieth century. *Journal of Geophysical Research*, 90(D4), 6181–6194. https://doi.org/10.1029/JD090iD04p06181
- Changnon, S. A. (2001). Assessment of the quality of thunderstorm data at first-order stations. *Journal of Applied Meteorology*, 40(4), 783–794. https://doi.org/10.1175/1520-0450(2001)040<0783:AOTQOT>2.0.CO;2
- Changnon, S. A., & Changnon, D. (2001). Long-term fluctuations in thunderstorm activity in the United States. Climatic Change, 50(4), 489–503. https://doi.org/10.1023/A:1010651512934
- Chen, S. M., Du, Y., & Fan, L. M. (2004). Lightning data observed with lightning location system in Guang-dong province, China. *IEEE Transactions on Power Delivery*, 19(3), 1148–1153. https://doi.org/10.1109/TPWRD.2004.829884
- Christian, H. J., Blakeslee, R. J., Boccippio, D. J., Boeck, W. L., Buechler, D. E., Driscoll, K. T., et al. (2003). Global frequency and distribution of lightning as observed from space by the Optical Transient Detector. *Journal of Geophysical Research*, 108(D1), 4005. https://doi.org/10.1029/2002JD002347
- Christian, H. J., Blakeslee, R. J., Goodman, S. J., Mach, D. A., Stewart, M. F., Buechler, D. E., et al. (1999). The lightning imaging sensor. In *Proceedings of the 11th International Conference on Atmospheric Electricity* (pp. 746–749). Guntersville, Alabama: NASA Conf. Publ.
- Chronis, T. G., Goodman, S. J., Cecil, D., Buechler, D., Robertson, F. J., Pittman, J., & Blakeslee, R. J. (2008). Global lightning activity from the ENSO perspective. *Geophysical Research Letters*, 35, L19804. https://doi.org/10.1029/2008GL034321
- Enno, S. E., Post, P., Briede, A., & Stankunaite, I. (2014). Long-term changes in the frequency of thunder days in the Baltic countries. *Boreal Environment Research*, 19(2014), 452–466.
- Finney, D. L., Doherty, R. M., Wild, O., Stevenson, D. S., MacKenzie, I. A., & Blyth, A. M. (2018). A projected decrease in lightning under climate change. *Nature Climate Change*, 8, 210–213.
- Fleagle, R. G. (1949). The audibility of thunder. The Journal of the Acoustical Society of America, 21(4), 411–412. https://doi.org/10.1121/1.1906528
- Ghavidel, Y., Baghbanan, P., & Farajzadeh, M. (2017). The spatial analysis of thunderstorm hazard in Iran. *Arabian Journal of Geosciences*, 10(5), 123.
- Goodman, S., Buechler, D., Knupp, K., Driscoll, K., & McCaul, E. (2000). The 1997–98 El Niño event and related wintertime lightning variations in the southeastern United States. *Geophysical Research Letters*, 27(4), 541–544. https://doi.org/10.1029/1999GL010808
- Goodman, S. J., Blakeslee, R. J., Koshak, W. J., Mach, D., Bailey, J., Buechler, D., et al. (2013). The GOES-R Geostationary Lightning Mapper (GLM). Atmospheric Research, 125-126, 34–49. https://doi.org/10.1016/j.atmosres.2013.01.006
- Goodman, S. J., & MacGorman, D. R. (1986). Cloud-to-ground lightning activity in mesoscale convective complexes. *Monthly Weather Review*, 114(12), 2320–2328. https://doi.org/10.1175/1520-0493(1986)114<2320:CTGLAI>2.0.CO;2
- Gorbatenko, V., & Dulzon, A. A. (2001). Variations of thunderstorm, Biology and Ecology, Korus.
- Grazulis, T. P., & Abbey, R. F. Jr. (1983, October). 103 years of violent tornadoes: Patterns of serendipity, population, and mesoscale topography. In *Preprints, 13th Conf. on Severe Local Storms* (pp. 124–127). Tulsa, OK: Amer. Meteor. Soc.
- Hamid, E. Y., Kawasaki, Z. I., & Mardiana, R. (2001). Impact of the 1997–98 El Niño event on lightning activity over Indonesia. *Geophysical Research Letters*, 28(1), 147–150. https://doi.org/10.1029/2000GL011374
- Kitagawa, N. (1989). Long-term variations in thunder-day frequencies in Japan. *Journal of Geophysical Research*, 94(D11), 13,183–13,189. https://doi.org/10.1029/JD094iD11p13183
- Kunz, M., Sander, J., & Kottmeier, C. (2009). Recent trends of thunderstorm and hailstorm frequency and their relation to atmospheric characteristics in southwest Germany. *International Journal of Climatology*, 29(15), 2283–2297. https://doi.org/10.1002/joc.1865
- Lavigne, T., Liu, C., Deierling, W., & Mach, D. (2017). Relationship between the global electric circuit and electrified cloud parameters at diurnal, seasonal, and interannual timescales. *Journal of Geophysical Research: Atmospheres*, 122, 8525–8542. https://doi.org/10.1002/ 2016JD026442
- Lin-Lin, Z., Jian-Hua, S., & Jie, W. (2010). Thunder events in China: 1980–2008. Atmospheric and Oceanic Science Letters, 3(4), 181–188. https://doi.org/10.1080/16742834.2010.11446866
- Liu, C., Cecil, D. J., Zipser, E. J., Kronfeld, K., & Robertson, R. (2012). Relationships between lightning flash rates and radar reflectivity vertical structures in thunderstorms over the tropics and subtropics. *Journal of Geophysical Research*, 117, D06212. https://doi.org/ 10.1029/2011JD017123
- Liu, C., Williams, E. R., Zipser, E. J., & Burns, G. (2010). Diurnal variations of global thunderstorms and electrified shower clouds and their contribution to the global electrical circuit. *Journal of the Atmospheric Sciences*, 67(2), 309–323. https://doi.org/10.1175/ 20091AS3248 1
- Liu, C., & Zipser, E. J. (2015). The global distribution of largest, deepest, and most intense precipitation systems. *Geophysical Research Letters*, 42, 3591–3595. https://doi.org/10.1002/2015GL063776
- Liu, N., & Liu, C. (2016). Global distribution of deep convection reaching tropopause in 1 year GPM observations. *Journal of Geophysical Research: Atmospheres*, 121, 3824–3842. https://doi.org/10.1002/2015JD024430
- Mackerras, D., Darveniza, M., Orville, R. E., Williams, E. R., & Goodman, S. J. (1998). Global lightning: Total, cloud and ground flash estimates. *Journal of Geophysical Research*, 103(D16), 19,791–19,809. https://doi.org/10.1029/98JD01461
- Merenti-Välimäki, H. L., Lönnqvist, J., & Laininen, P. (2001). Present weather: Comparing human observations and one type of automated sensor. *Meteorological Applications*, 8(4), 491–496. https://doi.org/10.1017/S1350482701004108
- Negri, A. J., Bell, T. L., & Xu, L. (2002). Sampling of the diurnal cycle of precipitation using TRMM. Journal of Atmospheric and Oceanic Technology, 19(9), 1333–1344. https://doi.org/10.1175/1520-0426(2002)019<1333:SOTDCO>2.0.CO;2
- Ni, X., Zhang, Q., Liu, C., Li, X., Zou, T., Lin, J., et al. (2017). Decreased hail size in China since 1980. Scientific Reports, 7(1), 10913. https://doi.org/10.1038/s41598-017-11395-7
- Pinto, O. (2015). Thunderstorm climatology of Brazil: ENSO and tropical Atlantic connections. *International Journal of Climatology*, 35(6), 871–878. https://doi.org/10.1002/joc.4022
- Pinto, O., Pinto, I. R. C. A., & Ferro, M. A. S. (2013). A study of the long-term variability of thunderstorm days in southeast Brazil. *Journal of Geophysical Research: Atmospheres*, 118, 5231–5246. https://doi.org/10.1002/jgrd.50282



- Price, C., & Rind, D. (1994). Possible implications of global climate change on global lightning distributions and frequencies. *Journal of Geophysical Research*, 99(D5), 10.823–10.831. https://doi.org/10.1029/94JD00019
- Price, C. G. (2013). Lightning applications in weather and climate research. Surveys in Geophysics, 34(6), 755–767. https://doi.org/10.1007/s10712-012-9218-7
- Reeve, N., & Toumi, R. (1999). Lightning activity as an indicator of climate change. Quarterly Journal of the Royal Meteorological Society, 125(555), 893–903. https://doi.org/10.1002/qj.49712555507
- Rudlosky, S. D., Goodman, S. J., Virts, K. S., & Bruning, E. C. (2019). Initial geostationary lightning mapper observations. *Geophysical Research Letters*, 46, 1097–1104. https://doi.org/10.1029/2018GL081052
- Sátori, G., Williams, E., & Lemperger, I. (2009). Variability of global lightning activity on the ENSO time scale. *Atmospheric Research*, 91(2–4), 500–507. https://doi.org/10.1016/j.atmosres.2008.06.014
- Schaefer, J. T., & Galway, J. G. (1982). *Population biases in tornado climatology*. Preprints, 12th Conference on Severe Local Storms (pp. 51–54.). San Antonio, TX: Amer. Meteor. Soc.
- Seto, S., Iguchi, T., & Oki, T. (2013). The basic performance of a precipitation retrieval algorithm for the global precipitation measurement mission's single/dual-frequency radar measurements. *IEEE Transactions on Geoscience and Remote Sensing*, 51(12), 5239–5251. https://doi.org/10.1109/TGRS.2012.2231686
- Sonnadara, U. (2016). Spatial and temporal variations of thunderstorm activities over Sri Lanka. *Theoretical and Applied Climatology*, 124(3–4), 621–628. https://doi.org/10.1007/s00704-015-1442-x
- Toracinta, E. R., Cecil, D. J., Zipser, E. J., & Nesbitt, S. W. (2002). Radar, passive microwave, and lightning characteristics of precipitating systems in the tropics. *Monthly Weather Review*, 130(4), 802–824. https://doi.org/10.1175/1520-0493(2002)130<0802:RPMALC>2.0.
- Tuomi, T. J., & Mäkelä, A. (2008). Thunderstorm climate of Finland 1998-2007. Geophysica, 44, 29-42.
- Williams, E. (2005). Lightning and climate: A review. Atmospheric Research, 76(1-4), 272–287. https://doi.org/10.1016/j. atmosres.2004.11.014
- Williams, E., Rothkin, K., Stevenson, D., & Boccippio, D. (2000). Global lightning variations caused by changes in thunderstorm flash rate and by changes in the number of thunderstorms. *Journal of Applied Meteorology*, 39(12), 2223–2230. https://doi.org/10.1175/1520-0450(2001)040<2223:GLVCBC>2.0.CO;2
- Williams, E. R. (1992). The Schumann resonance: A global tropical thermometer. Science, 256(5060), 1184–1187. https://doi.org/10.1126/science.256.5060.1184
- Williams, E. R. (1994). Global circuit response to seasonal variations in global surface air temperature. *Monthly Weather Review*, 122(8), 1917–1929. https://doi.org/10.1175/1520-0493(1994)122<1917:GCRTSV>2.0.CO;2
- Williams, E. R. (1999). Global circuit response to temperature on distinct time scales: A status report. In M. Hayakawa (Ed.), Atmospheric and Ionospheric Electromagnetic Phenomena Associated With Earthquakes. Tokyo: Terra Sci.
- Williams, E. R. (2009). The global electrical circuit: A review. Atmospheric Research, 91(2-4), 140-152. https://doi.org/10.1016/j. atmosres 2008 05 018
- Williams, E. R. (2012). Franklin lecture: Lightning and climate. Retrieved from http://fallmeeting.agu.org/2012/events/franklinlecture-ae31a-lightning-and-climate-video-on-demand/
- Williams, E. R., & Heckman, S. J. (1993). The local diurnal variation of cloud electrification and the global diurnal variation of negative charge on the Earth. Journal of Geophysical Research, 98(D3), 5221–5234. https://doi.org/10.1029/92JD02642
- World Meteorological Organization (1953). World distribution of thunderstorm days. Part 1: Tables. Geneva, Switzerland: WMO Publ. 21, TP 6. Ye, H., Fetzer, E. J., Wong, S., Lambrigtsen, B. H., Wang, T., Chen, L., & Dang, V. (2017). More frequent showers and thunderstorm days under a warming climate: Evidence observed over Northern Eurasia from 1966 to 2000. Climate Dynamics, 49(5–6), 1933–1944. https://doi.org/10.1007/s00382-016-3412-0
- Yoshida, S., Morimoto, T., Ushio, T., & Kawasaki, Z. (2007). ENSO and convective activities in Southeast Asia and western Pacific. Geophysical Research Letters, 34, L21806. https://doi.org/10.1029/2007GL030758
- Zhang, Q., Ni, X., & Zhang, F. (2017). Decreasing trend in severe weather occurrence over China during the past 50 years. *Scientific Reports*, 7(1), 42310. https://doi.org/10.1038/srep42310
- Zipser, E. J., Cecil, D. J., Liu, C., Nesbitt, S. W., & Yorty, D. P. (2006). Where are the most intense thunderstorms on Earth? *Bulletin of the American Meteorological Society*, 87(8), 1057–1072. https://doi.org/10.1175/BAMS-87-8-1057